HHS Public Access

Author manuscript

Microcirculation. Author manuscript; available in PMC 2016 May 02.

Published in final edited form as:

Microcirculation. 2013 February ; 20(2): 158–169. doi:10.1111/micc.12014.

Air Pollution Particulate Matter Collected from an Appalachian Mountaintop Mining Site Induces Microvascular Dysfunction

TRAVIS L. KNUCKLES[*,†], **PHOEBE A. STAPLETON**[*,†], **VALERIE C. MINARCHICK**[†], **LAURA ESCH**[‡], **MICHAEL MCCAWLEY**[‡], **MICHAEL HENDRYX**[‡], and **TIMOTHY R. NURKIEWICZ**[*,†,§]

[*]Center for Cardiovascular and Respiratory Sciences, West Virginia University School of Medicine, Morgantown, West Virginia, USA

[†]Department of Physiology and Pharmacology, West Virginia University School of Medicine, Morgantown, West Virginia, USA

[‡]Department of Community Medicine, West Virginia University School of Medicine, Morgantown, West Virginia, USA

[§]Department of Neurobiology and Anatomy, West Virginia University School of Medicine, Morgantown, West Virginia, USA

Abstract

Objective—Air pollution PM is associated with cardiovascular morbidity and mortality. In Appalachia, PM from mining may represent a health burden to this sensitive population that leads the nation in cardiovascular disease, among others. Cardiovascular consequences following inhalation of PM_{MTM} are unclear, but must be identified to establish causal effects.

Methods—PM was collected within 1 mile of an active MTM site in southern WV. The PM was extracted and was primarily <10μ_M in diameter (PM_{10}), consisting largely of sulfur (38%) and silica (24%). Adult male rats were IT with 300 μg PM_{MTM}. Twenty-four hours following exposure, rats were prepared for intravital microscopy, or isolated arteriole experiments.

Results—PM_{MTM} exposure blunted endothelium-dependent dilation in mesenteric and coronary arterioles by 26%, and 25%, respectively, as well as endothelium-independent dilation. *In vivo*, PM_{MTM} exposure inhibited endothelium-dependent arteriolar dilation (60% reduction). α-adrenergic receptor blockade inhibited PVNS-induced vasoconstriction in exposed animals compared with sham.

Conclusions—These data suggest that PM_{MTM} exposure impairs microvascular function in disparate microvascular beds, through alterations in NO-mediated dilation and sympathetic nerve influences. Microvascular dysfunction may contribute to cardiovascular disease in regions with MTM sites.

Address for correspondence: Timothy R. Nurkiewicz, Ph.D., Center for Cardiovascular and Respiratory Sciences, Robert C. Byrd Health Sciences Center, 1 Medical Center Drive, West Virginia University, Morgantown, WV 26506, USA. tnurkiewicz@hsc.wvu.edu.

Keywords

air pollution particulate matter; circulation; endothelial dysfunction; cardiovascular disease; mountaintop mining

INTRODUCTION

PM is associated with excess cardiovascular morbidity and mortality [12,38]. Appalachia is an economically depressed and isolated region spanning parts of 13 states stretching from northeastern Mississippi, to southwestern New York, and encompassing the entire state of WV [2]. In WV, health disparities, most notably cardiovascular disease, have been demonstrated to be more prominent in counties where major coal mining activities are present compared with non-mining counties [15,20]. These health issues as well as environmental impacts have taken center stage as reports of the deleterious effects of MTM are being reported [22]. Moreover, published work has strongly tied cardiovascular health effects to the mass of coal extracted compared with similar non-mining areas [20,21]. Additionally, these cardiovascular health effects have been strongly linked to active MTM areas [15]. These findings suggest that toxicants and environmental stressors associated with MTM negatively affect communities proximal to these mines.

As with all mining operations, MTM site operators are required to abate fugitive dust generation in open mine areas [1]. However, abatement is not required for fugitive dust generated by blasting and combustion particulates from heavy equipment. Hence, PM may represent a significant toxicant generated by active MTM sites [17]. PM mortality has been demonstrated over a wide variety of geographical locales [12]. By source, PM derived from combustion appears to possess the greatest toxicity of ambient sources [10]. While size is a strong predictor of cardiovascular toxicity [43], coarse PM exposures also have been associated with cardiovascular morbidity and mortality [13]. There is a lack of literature pertaining to PM_{MTM}; however, a good corollary can be drawn between PM_{MTM} and PM produced by opencast mining [17,23]. Opencast mining PM contains largely the geological and mineralogical composition of the mine, and a significant portion of combustion source particulates, with little coal dust in the total sample [23]. Hence, PM_{MTM} used in this study would predictably contain a great deal of crustal material and combustion source PM, the latter of which a significant database of untoward health effects exists [29,38].

While this knowledge is critical for making the initial speculations on analogous health outcomes, it does little to illuminate the underlying mechanisms of microvascular relationships. The microcirculation is the primary site of vascular resistance and nutrient and waste exchange in the body. Perturbations in microvascular vasoreactivity can have profound impact on tissue perfusion, and ultimately homeostasis [41]. Deficits in tissue perfusion through microvascular dysfunction can eventually lead to ischemia. Indeed, several cardiovascular conditions that are ultimately the result of microvascular dysfunction and pathology are angina, myocardial infarction [3], stroke [42], and hypertension [45]. Microvascular dysfunction is probably not isolated to a particular vascular bed, but occurring simultaneously throughout the body [42]. Hence, the complex mechanisms

involved in microvascular function that controls tissue specific perfusion are of paramount importance with regard to the systemic microvascular effects that follow PM exposure.

Given that tissues probably develop microvascular dys-function in concert, the purpose of this study was to evaluate underlying mechanisms of arteriolar function in disparate systemic microvascular beds following PM_{MTM} exposure. We hypothesized that PM_{MTM} exposure alters arteriolar reactivity through mechanistic pathways involved in endothelium-dependent arteriolar dilation, particularly NO-mediated dilation, and that these alterations in vasoreactivity would vary by vascular bed.

MATERIALS AND METHODS

Animals

Male Sprague–Dawley rats (6–11 weeks old) were purchased from Hilltop Labs and housed at the WV University Health Sciences Center. Animal vital statistics are shown in Table 1. An N of 17 sham and 13 PM_{MTM}-exposed animals were used for the intravital preparation, and an N of 11 sham and 8 PM_{MTM}-exposed animals were used for the isolated arteriole preparation (Table 1). All animal procedures were approved by the WVU Institutional Animal Care and Use Committee.

PM_{MTM}

Air was sampled at two sites within 1 mile of an active MTM site (Sundial, WV, USA). PM was collected on 35 mm 5μ_M pore size PTFE fiber-backed filters (Whatman, Springfield Mill, UK, Figure 1A) for 2–4 weeks. Air flow rate across the filters averaged 12 L/min. Following collection, the filters were stored at room temperature (20–25°C) and ambient humidity (10–30%) in the dark for 0.5–1 year prior to extraction. PM (Figure 1B) was removed from the filters by gentle agitation in 15 mL of ultrapure water (Cayman Chemical, Ann Arbor, MI, USA) in a glass jar for 96 hours. Storage and extraction of the particles from the filters are consistent with previously reported methods [14]. Aliquots of the particle suspension were dried down in 2 mL cryovials for 18 hours in a Speedvac (Savant, Midland, MI, USA). Total particle weight was determined by a microbalance (Metler-Toledo, Columbus, OH, USA).

PM_{MTM} Metal, Sulfate, and Carbon Analysis

SEM-EDX spectroscopy—Elemental concentration in atomic weight (ppm) was obtained from individual particles with a SEM (JEOL LTD., Tokyo, Japan) coupled with EDX technology (Oxford Instruments, Oxfordshire, UK). A filter sample (~2 cm^2) was obtained from a PTFE filter and mounted with double-sided adhesive copper tape on a brass (Cu and Zn) specimen stub. Approximately four to five samples per filter and 20–25 individual particles per sample were randomly chosen for a total analysis of 100 particles per filter using the Spot & ID EDX Analysis Mode. An accelerating voltage of 20 kV was used and the working distance was set to 15 mm with a 120 seconds live time for X-ray acquisition. Particles 0.5–20μ_M were analyzed and a quant optimization was performed on Cu.

ICP-AES/IC—Analyses were performed on the PM_{MTM} by a commercial laboratory (RTI International, RTP, NC, USA). Briefly, pre-weighed PM_{MTM} was resuspended into 5 mL of methanol and vortexed. The sample was then split into two equal volume aliquots for ICP-AES and IC analysis. ICP-AES analysis was performed via EPA method 3060C on material extracted using EPA method 3052. Sulfate IC analysis was performed by EPA method 300.0 with modifications for use on the Dionex ICS-3000 (Thermo Scientific, Sunnyvale, CA, USA) with eluent generation [44]. Standard reference material 1648a (St. Louis, MO, US Urban PM; NIST, Gaithersburg, MD, USA) was used as a quality control. The following metals and compounds were determined: Al, Ba, Ca, Co, Cr, Cu, Fe, K, Mg, Mn, Na, Ni, Pb, Si, Sn, Ti, V, Zn, and SO_4. Elements not appearing in Table 2 were below detectable limits. OC and EC were analyzed using an OC/EC Analyzer (Sunset Laboratories, Hillsburough, NC, USA) by RTI International. A 0.025 mL aliquot of PM_{MTM} resuspended in methanol, as above, was loaded onto a 1.49 cm^2 quartz punch along with a duplicate and blank. Total OC/EC were calculated from the resulting spectra, as previously described [4].

IT Exposure

IT was performed as previously described [35]. Briefly, extracted PM_{MTM} samples were resuspended in sterile saline (Normosol®-R, Hospira, Lake Forest, IL, USA) with 5% fetal bovine serum via sonication for 30 seconds. Rats were briefly anesthetized (isoflurane gas) and instilled with 0.3 mL of vehicle or vehicle with 300 μg of PM_{MTM}. Twenty-four hours following instillation, mesenteric and coronary arterioles were isolated or intravital microscopy was performed.

Intravital Microscopy

Intravital microscopy was performed as previously described [24]. Briefly, rats were anesthetized by an i.p. injection of Inactin (100 mg/kg) and maintained at 37°C. The trachea was intubated to ensure a patent airway, and the right carotid artery was cannulated to measure arterial pressure. The right spinotrapezius muscle was exteriorized for microscopic observation over a clear pedestal, leaving all feed arteries and innervations intact. The tissue bath was continuously superfused with an electrolyte solution ([in m_M] 119 NaCl, 25 $NaHCO_3$, 6 KCl, and 3.6 $CaCl_2$, pH 7.4, 290 mOsm), warmed to 35°C, and equilibrated with 95% N_2, 5% CO_2 with a superfusion flow rate of 4–6 mL/min. The preparation was then transferred to the stage of an Olympus intravital microscope coupled to a CCD camera and was observed under a 20× water immersion objective (final image magnification was 743×). Greater than three images were digitally captured via DP controller (Olympus, Center Valley, PA, USA) during a baseline period and immediately following each experimental period. Arteriolar diameters from each digital image were measured with Microsuite analysis software (Olympus). Steady-state arteriolar diameters were averaged per experimental period to reduce sampling variability [24].

Isolated Arterioles

Coronary arterioles were isolated as previously described [26,27]. Arterioles from the mesentery were also removed in a similar manner. Briefly, the heart or the mesentery was removed from isoflurane anesthetized animals and placed into a silastic-coated dish

containing chilled (4°C) PSS (in mM; 129.8 NaCl, 5.4 KCl, 1.1 NaH_2PO_4, 1.7 $MgCl_2$, 19.0 $NaHCO_3$, 1.8 $CaCl_2$, and 5.5 glucose, pH 7.4, 290 mOsm). The heart was flushed of excess blood and the LAD artery was located. Arterioles ≤170 μM, which corresponded to third to fourth order arterioles in the heart or fourth and fifth order arterioles in the mesentery, were isolated and transferred to a vessel chamber containing fresh PSS oxygenated with normoxic gas (21% O_2–5% CO_2–74% N_2), cannulated with glass micropipettes, and secured with nylon suture (10–0 ophthalmic; Alcon, Hemel Hempstead, UK). Arterioles were pressurized to 45 mmHg (coronary) or 80 mmHg (mesentery) with PSS using a servo controlled peristaltic pump (Living Systems Instrumentation, Burlington, VT, USA) without flow and superfused with oxygenated 37°C PSS at a rate of 10 mL/min. Vessel diameter was measured with a video caliper (Colorado Video, Boulder, CO, USA). Vessels without leaks were allowed to develop spontaneous tone (≥17% less initial diameter). Ca^{++}-free PSS was superfused at the end of all experiments to determine passive arteriolar diameters.

Chemicals

Intravital microscopy—Compounds were introduced via a syringe pump and at concentrations that previously described elsewhere [24]. A23187, a calcium ionophore, was introduced into the lumen of the arterioles at a concentration of 1 μM, as previously described [36]. L-NMMA (Calbiochem, Gibbstown, NJ, USA) was used at a final tissue bath concentration of 0.1 mM to competitively inhibit NOS activity. The superfusate concentration of phentolamine, an α-adrenergic receptor blocker, was 1 μM. ADO was superfused at the end of all experiments (0.1 mM) to determine passive arteriolar diameters.

Isolated arteriole studies—Compounds were added directly to the superfusate solution as previously described [26,27]. ACh, Spermine NONOate, and PE, were added at increasing concentrations of 0.001–100 μM or A23187 1–1000 nM. All chemicals were from Sigma (St. Louis, MO, USA), unless otherwise noted.

Statistics and Formulas

Intravital microscopy—Arteriolar diameter, D (μM), was recorded during a control, intraluminal infusion or PVNS period and immediately following AH. Resting vascular tone was calculated by: %tone = $[(D_{pass} - D_c)/D_{pass}] \times 100$, where D_{pass} is passive diameter under ADO and D_c is the diameter measured during the control period. Arteriolar responses were normalized as follows: percent change from control = $[(D_{ss}/D_c) - 1] \times 100$, where D_{ss} is the steady-state diameter following intraluminal infusion, AH, and PVNS. D_c immediately prior to the beginning of any experimental procedure was used to calculate %tone and reported as 0 PSI diameter measurements in the A23187 experimental series. All data are reported as mean ± SE.

Isolated arteriole studies—Spontaneous tone was calculated by: % tone = $[(D_{pass} - D_I)/D_{pass}] \times 100$, where D_{pass} is the maximal diameter recorded under Ca^{++} free PSS for coronary or mesenteric arterioles, respectively. D_I is the initial diameter of the arteriole prior to the experimental period. Active responses to pressure changes were normalized to the maximal diameter according to the following formula: % Normalized diameter = $[(D_{ss}/D_{pass})] \times 100$, D_{ss} is the steady-state diameter during each pressure step. The experimental

responses to ACh, A23187, and Spermine NONOate are expressed using the following equation: % relaxation = $[(D_{ss} - D_{con})/(D_{pass} - D_{con})] \times 100$, where D_{ss} is the steady-state arteriolar diameter during the experimental period, D_{con} is the control diameter recorded immediately prior to experimental period. Responses to PE were calculated by the following formula: % constriction = $[(D_{ss} - D_{con})/(D_{con})] \times 100$. All experimental periods were two minutes in duration, and all steady-state diameters were collected for at least one minute [26,27].

Two-way repeated measures ANOVA was used to determine the effects of group, treatment, and group–treatment interactions on measured variables (Sigmastat, Chicago, IL, USA). For all ANOVA procedures, Student–Newman–Keuls *post hoc* analysis was used to identify pair-wise differences among specific groups. Significance was assessed at $p < 0.05$.

Experimental Protocols

Protocol 1—PVNS was performed on arcade bridge arterioles to determine responsiveness to sympathetic nerve stimulation [24]. These arterioles, originating from the thoracodorsal and 11th intercostal arteries, are the site of the majority of vascular resistance in the spinotrapezius muscle and hence of major importance in regulation of blood flow in the muscle [5]. A beveled micropipette was filled with 0.9% saline, attached to a Grass Stimulator (Model S9; Grass Instruments, Quincy, MA, USA), and the tip was brought to gently rest in the arteriolar adventitia. The perivascular nerves were stimulated between 20 and 60 seconds to develop stable constriction at a random frequency of 2–16 Hz. The observation site was distal to the stimulation site by 2–5 mm in the direction of flow. Microvascular reactivity was assessed first under normal superfusate conditions, then in the presence of phentolamine (1 μ_M). Arterioles were allowed to recover greater than two minutes between stimulations to return to baseline diameter.

Protocol 2—AH was induced in a separate set of rats through the stimulation of muscular contraction to determine the impact of PM_{MTM} exposure on metabolically induced vasodilation as previously described [24]. Briefly, electrodes were attached to the rostral and caudal ends of the muscle and attached to a Grass Stimulator. Muscular contraction was induced at a frequency of 2–12 Hz randomly for one minute. The L-NMMA was added following normal superfusate responses. Arterioles were allowed to recover greater than two minutes between stimulations to return to baseline diameter.

Protocol 3—Intraluminal infusion was performed on a separate set of rats as previously described [35]. Briefly, a micropipette was positioned in line with the stream of blood within an arcade bridge arteriole. Following an acclimation period, ejection of A23187 was performed for three minutes at 10–40 PSI via a Picospritzer II (World Precision Instruments Inc., Sarasota, FL, USA).

Protocol 4—Isolated mesenteric or coronary arteries were equilibrated until the vessels achieved spontaneous tone, then myogenic responsiveness was determined from 0–90 mmHg (coronary) and 0–105 mmHg (mesenteric) in 15 mmHg increments as previously described [26,27]. Endothelium-dependent arteriolar dilation was assessed with ACh and

A23187. NO sensitivity was assessed with the NO donor Spermine NONOate. Adrenergic sensitivity was assessed with PE. Following the addition of each agent, a washout period was performed to allow the vessel to return to basal tone prior to the addition of the next vasoactive agent.

RESULTS

Animal Characteristics

The animals used for the isolated arteriole experiments were significantly larger than those used for the intravital preparation (Table 1). There were no differences between MAP and HR between exposure groups (Table 1).

PM_{MTM} Characteristics

SEM-EDX analysis—Extracted PM_{MTM} (Figure 1C) was analyzed by SEM-EDX for major elements. The PM content was mostly found to contain sulfur (S, 38%) and silica (Si, 24%) by weight (wt/wt, Figure 1D), excluding carbon, oxygen and fluorine (the measured component of the filter backing). Outside of Si and S, the majority of the mass was made of alkali metals (sodium [Na], potassium [K]), alkali earth metals (calcium [Ca], magnesium [Mg]), transition metals (titanium [Ti], zinc [Zn], iron [Fe], copper [Cu], molybdenum [Mo]), and aluminum (Al).

ICP-AES/IC analysis—Metal analysis of the extracted PM_{MTM} revealed the highest abundant metal to be Ca^{2+} followed by Na^{+}. Si was not detected in the sample due to poor recovery ability of the procedure, as Si determination in the NIST 1648 control was 79% of actual (data not shown). Sulfate was highly represented in the sample at 92 μg/mg or 9% of the sample. Total metal and sulfate analysis constituted ~11% of the total mass of the sample. Measured OC was ~27% of the sample at 274.6 μg/mg and was the highest component of the particulate sample (Table 2). Furthermore, ranking of the elements based on abundance was relatively consistent between SEM-EDX and ICP-AES analyses with the exception of Cu^{++} and Si, which were not detected, and Na^{+} and Mg^{++}, which are out of order (Table 2).

Microvessel Characteristics

Arteriolar diameter and tone under normal superfusate conditions were not different between sham and PM_{MTM}-exposed animals in both *in vivo* and isolated vessels (Table 3). The various superfusate treatments did not alter arteriolar diameter or tone except for L-NMMA treatment in the PM_{MTM}-exposed group. Superfusion with L-NMMA significantly increased tone in the PM_{MTM} exposure group, but had no effect on diameter compared to sham-treated animals (Table 3). These data indicate that NO may have some role in modulation of resting tone following PM_{MTM} exposure.

Pulmonary PM_{MTM} Exposure Alters Arteriolar Reactivity *In Vivo*

To determine vasoreactivity through a similar mechanism across the various vascular beds in the *in vivo* or *in vitro* models, endothelium-dependent arteriolar dilation was induced through a predominantly NOS-mediated mechanism via the calcium ionophore A23187. In

sham animals, A23187 infusion induced a dose-dependent vasodilation that resulted in a near doubling of the arteriolar diameter (Figure 2A). Following PM_{MTM} exposure, A23187-induced vasodilation was completely inhibited and may have caused some slight but insignificant vasoconstriction (Figure 2A, 40 PSI). As a function of percent of control, the effect of PM_{MTM} exposure is striking with little to no increase in diameter compared with the control period in all three dose groups (Figure 2B).

Skeletal muscle arteriolar sensitivity to increased metabolic demand and endogenous sympathetic vasoconstrictors was evaluated by AH and PVNS, respectively (Figure 3). Vasodilation, induced by increased metabolic demand, was not different between sham and PM_{MTM}-exposed animals under normal superfusate conditions (max% 146 ± 12 sham, 165 ± 18 PM_{MTM}, Figure 3A). However, the addition of $_{L}$-NMMA, significantly blunted vasodilation in sham-treated animals, but not in PM_{MTM}-exposed animals (max% 88 ± 17 sham, 178 ± 25 PM_{MTM}, Figure 3A). These data suggest a greater reliance on compensatory mechanisms in the PM_{MTM}-exposed animals compared with sham. Perivascular nerves associated with arcade bridge arterioles were stimulated to determine the effect of pulmonary PM_{MTM} exposure on sympathetic nervous system responsiveness. Frequency-dependent decreases in diameter following PVNS were equivalent between arterioles from sham and PM_{MTM}-exposed animals (Figure 3B). The addition of phentolamine significantly blunted PVNS-mediated vasoconstriction in both sham and PM_{MTM}-exposed animals at 8 and 16 Hz (Figure 3B). Moreover, vasoconstriction was inhibited in PM_{MTM}-treated animals compared with sham at 8 Hz (max% −10 ± 5 sham, 7 ± 6 PM_{MTM}, Figure 3B). These data suggest that pulmonary exposure to PM_{MTM} shifts the balance of sympathetically mediated constriction toward a more adrenergic-dominated arteriolar constriction mediated by perivascular nerves, which could result from increased neurotransmitter release, receptor density, and/or receptor signaling.

Pulmonary PM_{MTM} Exposure Alters Arteriolar Reactivity *In Vitro*

To determine vasoreactivity changes in functionally distinct vascular beds, isolated arteriolar preparations were performed. As with intravital microscopy results, PM_{MTM} exposure significantly altered endothelium-dependent arteriolar dilation in isolated mesenteric and coronary arterioles (Figure 4). Vasodilation was significantly blunted at 1 μ_M A23187 in the coronary arterioles following PM_{MTM} IT compared with sham (max% 63 ± 7 sham, 38 ± 7 PM_{MTM}, Figure 4A). In the mesenteric arterioles, PM_{MTM} exposure significantly blunted A23187-induced vasodilation at 0.1– 1 μ_M doses compared with sham (max% 51 ± 4 sham, 25 ± 10 PM_{MTM}, Figure 4A). ACh-induced endothelium-dependent arteriolar dilation was also determined for both isolated mesenteric and coronary arterioles. Arteriolar vaso-dilation was blunted in both microvascular beds following PM_{MTM} exposure (Figure 4B). Coronary arterioles exhibited near complete inhibition of vasodilation to ACh (max% 57 ± 9 sham, 10 ± 11 PM_{MTM}, Figure 4B). Similarly, PM_{MTM} exposure significantly inhibited vasodilation in arterioles isolated from the mesentery of PM_{MTM}-exposed animals with a significant difference found at 0.1 μ_M and greater (max% 66 ± 6 sham, 29 ± 7 PM_{MTM}, Figure 4B). However, following PM_{MTM} exposure, arterioles were still somewhat responsive to ACh, as the 0.1 μ_M dose was significantly different from 1 and 10 n_M (Figure 4B). These data suggest

that pulmonary exposure to PM_{MTM} disrupts endothelium-dependent arteriolar dilation probably through inhibition of NO-mediated mechanisms.

To determine the effects of MTM pulmonary particle exposure on the vascular smooth muscle sensitivity to NO, endothelium-independent arteriolar dilation was determined with Spermine NONOate (Figure 5). PM_{MTM} exposure reduced overall vasodilation in coronary arterioles compared with sham-treated animals; however, individual doses of Spermine NONOate were not significantly ($p = 0.053$ at 10 n_M dose) different between exposure groups (max% 58 ± 7 sham, 46 ± 6 PM_{MTM}, Figure 5A). Furthermore, endothelium-independent arteriolar dilation was different following PM_{MTM} exposure in mesenteric arteries beginning at the 10 n_M (max% 70 ± 8 sham, 44 ± 8 PM_{MTM} Figure 5A). Myogenic responsiveness of coronary arterioles was not different between sham and PM_{MTM}-exposed animals (Figure 5B). However, at 105 mmHg arterioles from PM_{MTM}-exposed rats displayed a significantly greater myogenic response to the highest transmural pressure (Figure 5B). This probably suggests an enhanced vascular smooth muscle cell contractile responsiveness to transmural pressure; however, the biological relevance of this effect is unclear at present.

To determine the responsiveness of coronary and mesenteric arterioles to α-adrenergic stimulation, PE was performed. Neither coronary nor mesenteric arterioles showed any difference in reactivity to PE. Figure 6 depicts the maximal arteriolar constriction induced by PE in sham or PM_{MTM}-exposed rats.

DISCUSSION

This is the first study to demonstrate systemic microvascular effects of pulmonary exposure to particles collected near active MTM sites. Furthermore, this study demonstrates that pulmonary PM_{MTM} exposure results in acute microvascular dysfunction that (1) can be characterized across disparate vascular beds, (2) may be mediated through aberrant NO signaling, and (3) may also result from sympathetic nerve influences.

The particle composition reported in Figure 1D is consistent with a predominantly crustal particle sample. MTM sites are active areas of blasting, crushing, and grinding of materials that can blanket the surrounding areas with PM. In addition to mineralogical materials, engine exhaust emissions, likely off-road diesel, are normally thought to contribute to the overall PM burden. Indeed, particle characterization from opencast mines suggests a mix of natural and exhaust emissions with the mass dominated by geological PM [23]. However, based on our results of a high OC measurement with null amounts of EC, the overall composition would suggest a particulate largely composed of mineralogical dust and coal dust [4]. Preliminary particle monitoring from these sites suggests that, by total number, ultrafine to 0.2μm PM dominate the air sample (data not shown). This suggests that the bulk of the particles, by number, are anthropogenic in origin [46]. However, based on mass measurement (Figure 1D), the predominant particle composition is likely crustal.

Several studies have shown that, based on relative% of total mass, the compositional differences between rural and urban environments are minor, but significant, in terms of

differences in trace metal content and organic carbon [18,25]. However, the absolute content of Si in the eastern U.S. is quite low, whereas sulfate is the predominate non-carbon constituent [19]. In our particulate sample, the content of Si is second only to sulfate in terms of% of total mass. Si is a known respiratory toxicant and has been implicated in specific diseases in miners such as coal workers pneumoconiosis [7], which has been observed at surface mines in the United States [8]. Furthermore, silica particle exposures have been demonstrated to reduce HR variability measures in mice suggesting cardiotoxic effect [9].

The dosage of 300 μg per rat used in this study is a typical toxicological dosage to determine effect in healthy animals. Furthermore, this dosage, which is ~1 mg/kg, is lower than previous dosages used by our group [34], and lower than the dosages reported by other groups for initial determination of toxic effects [10]. Furthermore, the single-dose exposure in rats reported here would be equivalent to an accumulated dose over the course of 1.7 years based on ambient recorded concentrations of PM_{10} of 8.3 $\mu g/m^3$ a minute ventilation of 200 mL/min, and an estimated deposition fraction of 0.2. While high, these dosages represent an accumulated dosage based on a low average ambient particle concentrations that are approximately double that of ambient concentrations determined in non-mining areas (data not shown). Additionally, this study is a toxicological determination of an effect from which future work will determine dose response and temporal relationships.

Arteriolar tone, *in vivo*, is generated by the complex interplay between intrinsic and extrinsic factors [41]. In this study, PM_{MTM} exposure altered resting tone in the L-NMMA-treated arterioles (Table 3), which contrasts with previous findings in our laboratory [24]. Alteration of diameter or tone following L-NMMA treatment in the arteriolar network of the spinotrapezius is inconsistent between studies, with some investigations demonstrating an increase in arteriolar tone [28], while others show no change [24].

Metabolically stimulated vasodilation by AH was not found to be significantly different between the sham and PM_{MTM}-exposed groups (Figure 3A). These data are not consistent with previous exposures performed in our laboratory using TiO_2 nanoparticles in which we demonstrated a marked decrease in vasodilation at 12 Hz [24], suggesting that AH-mediated arteriolar dilation is not impaired following PM_{MTM} exposure. However, during NOS inhibition (L-NMMA), it becomes apparent that the mechanisms supporting AH after PM_{MTM} exposure are altered (Figure 3A). Because NOS inhibition did not affect AH in the PM_{MTM} group, other vasoactive influences, such as COX products, may be compensating to preserve normal reactivity to this metabolic stimulus. In previous work, we have demonstrated such a compensatory mechanism [24,27]. However, other metabolites of the arachidonic acid pathway may be involved in this mechanism [6]. Therefore, future studies directly evaluating changes in COX products, HETEs, ETEs, lipoxygenase products, and cytochrome P450 products, should be thoroughly tested to make definitive conclusions.

Endothelium-dependent arteriolar dilation was consistently blunted following PM_{MTM} exposure *in vivo* and *in vitro* (Figures 2 and 4). The overall arteriolar vasoreactivity to endothelium-dependent dilators is consistent with previous work from our laboratory with other particle sources [26,35]. However, as above, the mechanism of this effect, while likely

NO in origin, will require further investigation to fill out the pathways and mechanisms involved in the blunting of endothelium-dependent arteriolar following PM_{MTM} exposure.

Endothelium-independent arteriolar dilation has not been reported previously by our laboratory. However, in this study, arteriolar NO sensitivity was significantly impaired after PM_{MTM} exposure (Figure 5A). These data may suggest a shift not only in NO sensitivity but also in the activation of sGC, cyclic GMP and subsequent vasorelaxation [11]. Previous studies in humans using SNP corroborate the impairment in endothelium-independent arteriolar dilation following pulmonary pollutant exposures [32]. In this study, we opted for a spontaneous NO donor rather than a NO donor that requires interactions with sulfhydryl-containing molecules to release NO [40]. The spontaneous release of NO was not tissue mass-dependent, thus increasing the sensitivity of this assay.

In vivo, sympathetic afferents project into the arteriolar network down to the third to fourth order in the spinotrapezius muscle [30] and to the pre-capillary arterioles in the mesenteric network [16]. We found no difference in PVNS responsiveness following PM_{MTM} exposure (Figure 3B). However, the addition of the nonspecific α-adrenergic inhibitor, phentolamine, revealed a sensitivity to adrenergic blockade (Figure 3B), suggesting a possible switch from a “balanced” sympathetic-mediated constriction to a predominantly adrenergic mechanism. *In vitro*, no difference was found between control and PM_{MTM}-exposed arterioles with PE-induced vasoconstriction (Figure 6). The alteration in PVNS-induced vasoconstriction during α-adrenergic blockade is similar to previous work by our laboratory, which inferred an altered adrenergic signaling process that may be neuropeptide Y-mediated [24]. Furthermore, it is not clear whether or not the concentration of phentolamine used in this study (1 μ_M) produced a maximal inhibition of α-adrenergic receptor signaling [33]. Future work will focus on the effects of PM_{MTM} exposure on α-adrenergic and neuro-peptide Y transmitter expression within the local perivascular nerves, microvascular receptor density, as well as neuro-transmitter-induced vasoreactivity.

Overall, *in vivo* endothelium-dependent microvascular dysfunction (Figure 2) following PM_{MTM} exposure appears to be compensated for through other pathways (Figure 3), such that dysfunction is only revealed after the inclusion of an inhibitor. It is somewhat expected that in healthy animals, with redundant control mechanisms for microvascular tone, that microvascular reactivity under basal condition would not be perturbed. However, in disease models with significant pathology where these redundant pathways are diminished [31], the toxicity of PM has been shown to increase [39]. Furthermore, the epidemiological literature substantiates this in the fact that cardiovascular morbidity and mortality measures are greatest in the elderly, and in individuals with pre-existing conditions that probably possess a lower physiologic reserve compared with young healthy individuals [37].

We have demonstrated systemic microvascular dys-function following pulmonary PM_{MTM} exposure and the impairment is consistent in distinct tissues. This effect of PM_{MTM} exposure appears to be largely related to NO-mediated vasodilation, which may be functionally compensated for through other mechanisms, which our laboratory has demonstrated previously with exposure to nanoparticles [24]. This study also highlights the need for future work to undertake specific mechanistic changes to NO bioavailability, COX

product formation, among other enzymatic pathways in the microvasculature following PM_{MTM} exposure. As such, PM_{MTM} exposure appears to alter NO signaling mechanisms in the arteriolar network that have not been previously identified by our laboratory following exposure to particles. Hence, future work will focus on cGMP mimetics to determine what role MTM exposure has in vascular smooth muscle reactivity. Furthermore, sensitive populations in this region of Appalachia (e.g., the young and senescent) should be modeled appropriately to determine the degree to which PM_{MTM} exposure alters arteriolar dysfunction in these sensitive groups. Similarly, future studies will also include pathologies relevant to Appalachia (e.g., diabetes, hypertension, cardiovascular disease) to determine if PM_{MTM} exposure exacerbates arteriolar dysfunction with pre-existing disease. Future toxicological studies should also be performed to determine the relative toxicity of PM_{MTM} compared with other ambient PM sources that include samples from urban and rural airsheds as well as samples collected near opencast mines, with the purpose of identifying specific source components that may enhance the toxicity of PM_{MTM}.

PERSPECTIVE

Pulmonary PM exposure is a potent contributor to cardiovascular morbidity and mortality. PM point sources, such as MTM sites, can contribute significantly to the overall particle concentration. We have demonstrated that PM collected from populated areas with several active mine sites has the potential to adversely affect microvascular reactivity. This is the first investigation that has identified PM from MTM operations as a microvascular toxicant. If our findings translate into human outcomes, this may account or contribute to the known cardiovascular health disparities frequently observed in this unique population.

ACKNOWLEDGMENTS

The authors thank Mr. Carroll McBride (WVU), Dr. William Wonderlin (WVU), Mr. Frank Weber (RTI International), and Mr. John McGee (US EPA) for their expert technical assistance. We acknowledge the use of the WVU Shared Research Facilities.

FUNDING SOURCES

RO-1ES015022 and RC-1ES018274 (TRN), NSF-1003907 (VCM).

Abbreviations used

ACh	acetylcholine
ADO	adenosine
AH	active hyperemia
bpm	beats per minute
COX	cyclooxygenase
EDX	energy-dispersive X-ray
ETEs	eicosatetraenoates
HETEs	monohydroxy-eicosatetraenoic acids

HR	heart rate
IC	ion chromatography
ICP-AES	inductively coupled plasma atomic emission spectrometry
IT	intratracheal instillation
LAD	left anterior descending
L-NMMA	N^G-monomethyl-L-arginine
MAP	mean arterial pressure
MTM	mountaintop mining
NO	nitric oxide
NOS	NO synthase
PE	phenylephrine
PM	particulate matter
PM_{MTM}	MTM-derived PM
PM_{10}	PM < 10 μm
PSS	physiological saline solution
PTFE	polytetrafluoroethylene
PVNS	perivascular nerve stimulation
SEM	scanning electron microscope
sGC	soluble guanylyl cyclase
SNP	sodium nitroprusside
WV	West Virginia

REFERENCES

1. Stabilization of surface areas. 48 Federal Register. :11631983. 30 CFR 816.95.
2. [April 25, 2012] Appalachian Regional Commission. Moving Appalachia forward: Appalachian regional commissionstrategicplan2011–2016,2010. http://www.arc.gov/images/newsroom/publications/sp/ARCStrategicPlan2011-2016.pdf
3. Beltrame JF, Crea F, Camici P. Advances in coronary microvascular dysfunction. Heart Lung Circ. 2009; 18:19–27. [PubMed: 19119077]
4. Birch ME, Cary RA. Elemental carbon-based method for occupational monitoring of particulate diesel exhaust: methodology and exposure issues. Analyst. 1996; 121:1183–1190. [PubMed: 8831275]
5. Boegehold MA. Effect of salt-induced hypertension on microvascular pressures in skeletal muscle of Dahl rats. Am J Physiol. 1991; 260:H1819–H1825. [PubMed: 2058718]
7. Boushel R. Metabolic control of muscle blood flow during exercise in humans. Can J Appl Physiol. 2003; 28:754–773. [PubMed: 14710525]

7a. Castranova V, Vallyathan V. Silicosis and coal workers' pneumoconiosis. Environ Health Perspect. 2000; 108(Suppl. 4):675–684. [PubMed: 10931786]

8. Centers for Disease Control and Prevention. Pneumoconiosis and advanced occupational lung disease among surface coal miners–16 states, 2010–2011. MMWR Morb Mortal Wkly Rep. 2012; 61:431–434. [PubMed: 22695382]
9. Corey LM, Baker C, Luchtel DL. Heart-rate variability in the apolipoprotein E knockout transgenic mouse following exposure to Seattle particulate matter. J Toxicol Environ Health A. 2006; 69:953–965. [PubMed: 16728373]
10. Costa DL, Dreher KL. Bioavailable transition metals in particulate matter mediate cardiopulmonary injury in healthy and compromised animal models. Environ Health Perspect. 1997; 105(Suppl. 5):1053–1060. [PubMed: 9400700]
11. Craven PA, De Rubertis FR. Restoration of the responsiveness of purified guanylate cyclase to nitrosoguanidine, nitric oxide, and related activators by heme and heme-proteins. Evidence for involvement of the paramagnetic nitrosyl-heme complex in enzyme activation. J Biol Chem. 1978; 253:8433–8443. [PubMed: 30778]
12. Dockery DW, Pope CA III, Xu X, Spengler JD, Ware JH, Fay ME, Ferris BG Jr, Speizer FE. An association between air pollution and mortality in six U.S. cities. N Engl J Med. 1993; 329:1753–1759. [PubMed: 8179653]
13. Donaldson K, MacNee W. Potential mechanisms of adverse pulmonary and cardiovascular effects of particulate air pollution (PM10). Int J Hyg Environ Health. 2001; 203:411–415. [PubMed: 11556145]
14. Dye JA, Lehmann JR, McGee JK, Winsett DW, Ledbetter AD, Everitt JI, Ghio AJ, Costa DL. Acute pulmonary toxicity of particulate matter filter extracts in rats: coherence with epidemiologic studies in Utah Valley residents. Environ Health Perspect. 2001; 109(Suppl. 3):395–403. [PubMed: 11427389]
15. Esch L, Hendryx M. Chronic cardiovascular disease mortality in mountaintop mining areas of central Appalachian states. J Rural Health. 2011; 27:350–357. [PubMed: 21967378]
16. Furness JB. Arrangement of blood vessels and their relation with adrenergic nerves in the rat mesentery. J Anat. 1973; 115:347–364. [PubMed: 4586871]
17. Ghose MK, Majee SR. Characteristics of hazardous airborne dust around an Indian surface coal mining area. Environ Monit Assess. 2007; 130:17–25. [PubMed: 17285255]
18. Goetz S, Aneja VP, Zhang Y. Measurement, analysis, and modeling of fine particulate matter in eastern North Carolina. J Air Waste Manag Assoc. 2008; 58:1208–1214. [PubMed: 18817113]
19. Harrison RM, Yin J. Particulate matter in the atmosphere: which particle properties are important for its effects on health? Sci Total Environ. 2000; 249:85–101. [PubMed: 10813449]
20. Hendryx M. Mortality from heart, respiratory, and kidney disease in coal mining areas of Appalachia. Int Arch Occup Environ Health. 2009; 82:243–249. [PubMed: 18461350]
21. Hendryx M, Zullig KJ. Higher coronary heart disease and heart attack morbidity in Appalachian coal mining regions. Prev Med. 2009; 49:355–359. [PubMed: 19761789]
22. Holzman DC. Mountaintop removal mining: digging into Community Health concerns. Environ Health Perspect. 2011; 119:A476–A483. [PubMed: 22171378]
23. Jones T, Blackmore P, Leach M, Berube K, Sexton K, Richards R. Characterisation of airborne particles collected within and proximal to an opencast coalmine: South Wales, U.K. Environ Monit Assess. 2002; 75:293–312. [PubMed: 12004982]
24. Knuckles TL, Yi J, Frazer DG, Leonard HD, Chen BT, Castranova V, Nurkiewicz TR. Nanoparticle inhalation alters systemic arteriolar vasoreactivity through sympathetic and cyclooxygenase-mediated pathways. Nanotoxicology. 2012; 6:724–735. [PubMed: 21830860]
25. Laden F, Neas LM, Dockery DW, Schwartz J. Association of fine particulate matter from different sources with daily mortality in six U.S. cities. Environ Health Perspect. 2000; 108:941–947. [PubMed: 11049813]
26. LeBlanc AJ, Cumpston JL, Chen BT, Frazer D, Castranova V, Nurkiewicz TR. Nanoparticle inhalation impairs endothelium-dependent vasodilation in subepicardial arterioles. J Toxicol Environ Health A. 2009; 72:1576–1584. [PubMed: 20077232]
27. Le Blanc AJ, Moseley AM, Chen BT, Frazer D, Castranova V, Nurkiewicz TR. Nanoparticle inhalation impairs coronary microvascular reactivity via a local reactive oxygen species-dependent mechanism. Cardiovasc Toxicol. 2010; 10:27–36. [PubMed: 20033351]

28. Linderman JR, Boegehold MA. Modulation of arteriolar sympathetic constriction by local nitric oxide: onset during rapid juvenile growth. Microvasc Res. 1998; 56:192–202. [PubMed: 9828157]
29. Lundback M, Mills NL, Lucking A, Barath S, Donaldson K, Newby DE, Sandstrom T, Blomberg A. Experimental exposure to diesel exhaust increases arterial stiffness in man. Part Fibre Toxicol. 2009; 6:7. [PubMed: 19284640]
30. Marshall JM. The influence of the sympathetic nervous system on individual vessels of the microcirculation of skeletal muscle of the rat. J Physiol. 1982; 332:169–186. [PubMed: 7153926]
31. Marvar PJ, Nurkiewicz TR, Boegehold MA. Reduced arteriolar responses to skeletal muscle contraction after ingestion of a high salt diet. J Vasc Res. 2005; 42:226–236. [PubMed: 15855795]
32. Mills NL, Tornqvist H, Robinson SD, Gonzalez M, Darnley K, MacNee W, Boon NA, Donaldson K, Blomberg A, Sandstrom T, Newby DE. Diesel exhaust inhalation causes vascular dysfunction and impaired endogenous fibrinolysis. Circulation. 2005; 112:3930–3936. [PubMed: 16365212]
33. Naik JS, Xiang L, Hodnett BL, Hester RL. Alpha-adrenoceptor-mediated vasoconstriction is not involved in impaired functional vasodilation in the obese Zucker rat. Clin Exp Pharmacol Physiol. 2008; 35:611–616. [PubMed: 18177478]
34. Nurkiewicz TR, Porter DW, Barger M, Castranova V, Boegehold MA. Particulate matter exposure impairs systemic micro-vascular endothelium-dependent dilation. Environ Health Perspect. 2004; 112:1299–1306. [PubMed: 15345343]
35. Nurkiewicz TR, Porter DW, Barger M, Millecchia L, Rao KM, Marvar PJ, Hubbs AF, Castranova V, Boegehold MA. Systemic microvascular dysfunction and inflammation after pulmonary particulate matter exposure. Environ Health Perspect. 2006; 114:412–419. [PubMed: 16507465]
36. Nurkiewicz TR, Porter DW, Hubbs AF, Cumpston JL, Chen BT, Frazer DG, Castranova V. Nanoparticle inhalation augments particle-dependent systemic microvascular dysfunction. Part Fibre Toxicol. 2008; 5:1. [PubMed: 18269765]
37. Pope CA III. Epidemiology of fine particulate air pollution and human health: biologic mechanisms and who's at risk? Environ Health Perspect. 2000; 108(Suppl. 4):713–723. [PubMed: 10931790]
38. Pope CA III, Thun MJ, Namboodiri MM, Dockery DW, Evans JS, Speizer FE, Heath CW Jr. Particulate air pollution as a predictor of mortality in a prospective study of U. S. adults. Am J Respir Crit Care Med. 1995; 151:669–674. [PubMed: 7881654]
39. Proctor SD, Dreher KL, Kelly SE, Russell JC. Hypersensitivity of prediabetic JCR:LA-cp rats to fine airborne combustion particle-induced direct and noradrenergic-mediated vascular contraction. Toxicol Sci. 2006; 90:385–391. [PubMed: 16407093]
40. Salom JB, Barbera MD, Centeno JM, Orti M, Torregrosa G, Alborch E. Relaxant effects of sodium nitroprusside and NONO-ates in rabbit basilar artery. Pharmacology. 1998; 57:79–87. [PubMed: 9691227]
41. Segal SS. Regulation of blood flow in the microcirculation. Microcirculation. 2005; 12:33–45. [PubMed: 15804972]
42. Thompson CS, Hakim AM. Living beyond our physiological means: small vessel disease of the brain is an expression of a systemic failure in arteriolar function: a unifying hypothesis. Stroke. 2009; 40:e322–e330. [PubMed: 19228835]
43. Totlandsdal AI, Refsnes M, Skomedal T, Osnes JB, Schwarze PE, Lag M. Particle-induced cytokine responses in cardiac cell cultures—the effect of particles versus soluble mediators released by particle-exposed lung cells. Toxicol Sci. 2008; 106:233–241. [PubMed: 18700232]
44. US Environmental Protection Agency. 40 CFR 136 method 300.0: determination of inorganic anions by ion chromatography. 1993
45. Vicaut E. Microcirculation and arterial hyper-tension. Drugs 58 Spec. 1999; (1):1–11.
46. Wilson WE, Suh HH. Fine particles and coarse particles: concentration relation ships relevant to epidemiologic studies. J Air Waste Manag Assoc. 1997; 47:1238–1249. [PubMed: 9448515]

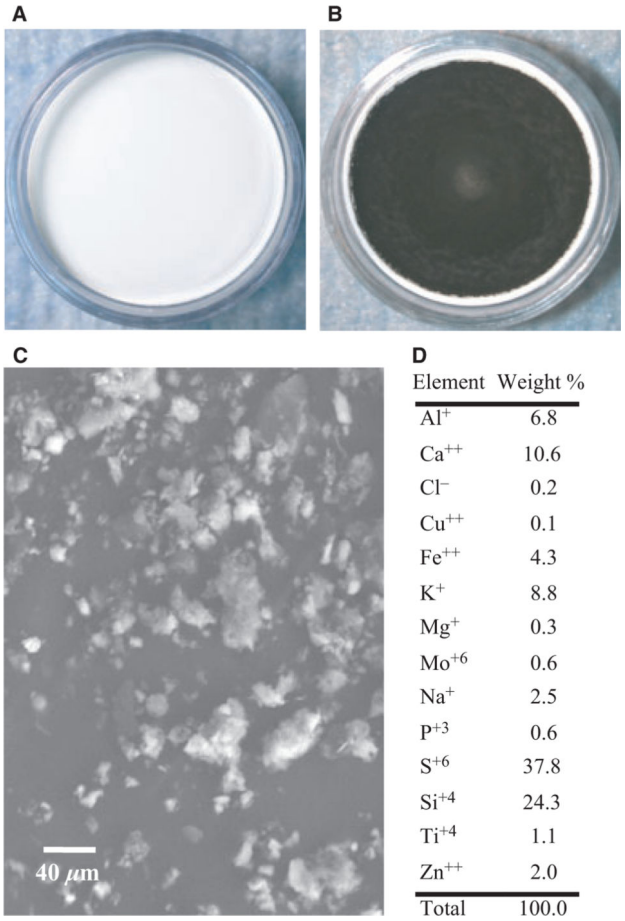

Element	Weight %
Al^{+}	6.8
Ca^{++}	10.6
Cl^{-}	0.2
Cu^{++}	0.1
Fe^{++}	4.3
K^{+}	8.8
Mg^{+}	0.3
Mo^{+6}	0.6
Na^{+}	2.5
P^{+3}	0.6
S^{+6}	37.8
Si^{+4}	24.3
Ti^{+4}	1.1
Zn^{++}	2.0
Total	100.0

Figure 1.

Collected PM_{MTM} with SEM and SEM-EDX compositional analysis. (**A**) Blank 35-mm filter loaded into the filter cassette. (**B**) A 35-mm filter following four weeks of sampling in an active MTM-area. (**C**) SEM image of the particle sample following extraction (see Methods). (**D**) The table of elements represents the SEM-EDX analysis of to determine the relative% by mass of selected elements. The sample consisted mostly of Si and S by weight.

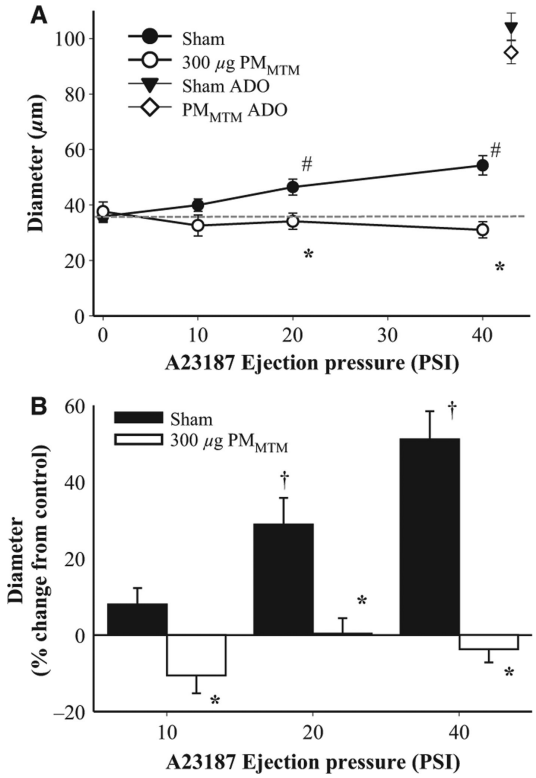

Figure 2.

PM_{MTM} exposure inhibits endothelium-dependent vasodilation in skeletal muscle arterioles *in vivo*. (**A**) Intraluminal infusion of A23187 (a calcium ionophore) led to a dose-dependent increase in arteriolar diameter. (**B**) Data from Panel (A) were analyzed using% change from control diameter (see Methods) to illustrate the dramatic difference between dilation in sham vs. PM_{MTM}-exposed arterioles. $^{*}p < 0.05$ vs. sham, $^{\#}p < 0.05$ vs. 0 PSI sham, $^{\dagger}p < 0.05$ vs. 10 PSI sham.

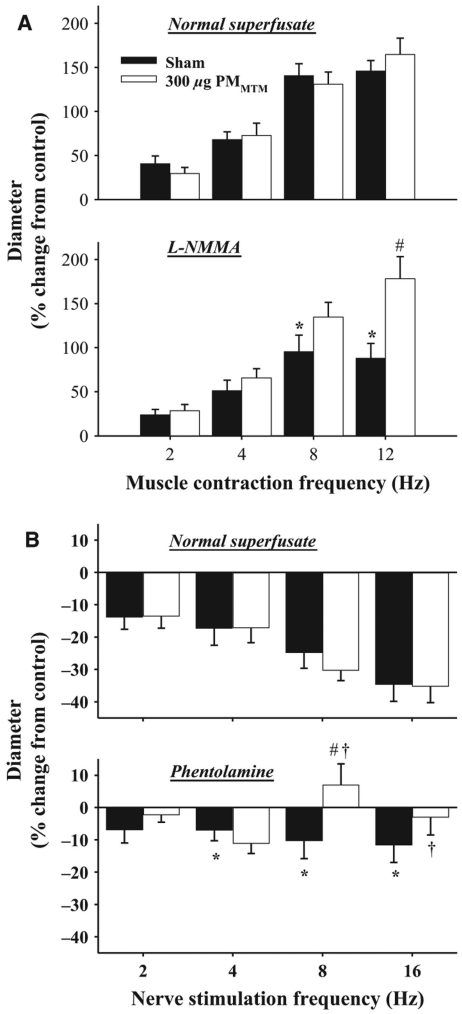

Figure 3.

PM$_{MTM}$ exposure alters vasoreactivity *in vivo*. (**A**) Panel (1): PM$_{MTM}$ exposure did not alter basal vasoreactivity to metabolic dilators. Panel (2): Inhibition of NOS impairs vasodilation in sham, but not in exposed animals following AH. (**B**) Panel (1): PM$_{MTM}$ exposure did not alter responsiveness to sympathetic arteriole constriction during normal PSS superfusion. Panel (2): PM$_{MTM}$ exposure increased sensitivity to α-adrenergic blockade during sympathetic arteriole constriction. $^{*}p < 0.05$ vs. normal superfusate at the same frequency, $^{\#}p < 0.05$ vs. sham. $^{\dagger}p < 0.05$ vs. PM$_{MTM}$-treated normal superfusate.

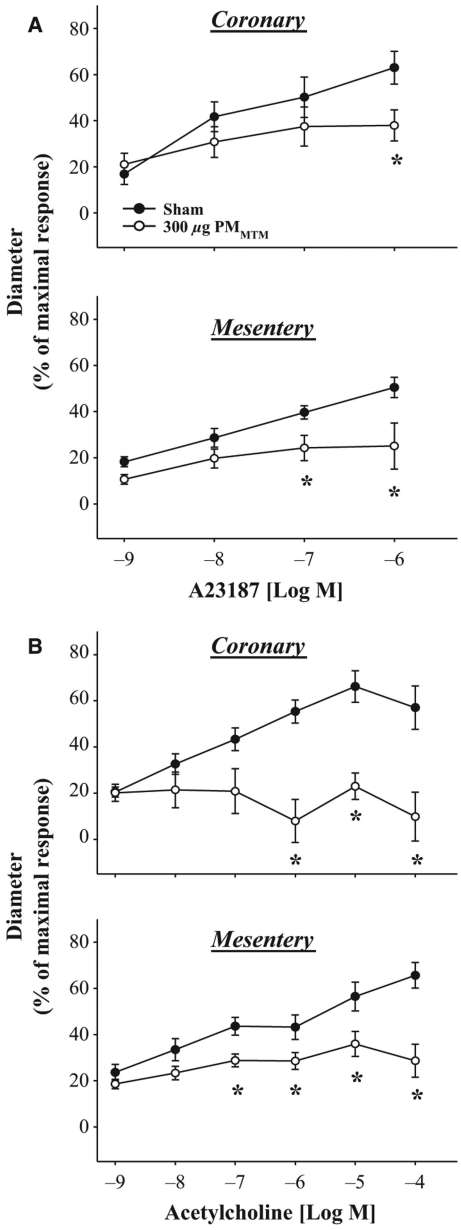

Figure 4.

In vitro responses to endothelium-dependent dilators in coronary and mesenteric arterioles. (**A**) Panel (1): Coronary arteriolar dose-dependent dilation to A23187 was inhibited following pulmonary exposure to PM_{MTM}. Panel (2): Similarly, mesenteric arteriolar dilation induced by A23187 was also inhibited following PM_{MTM} exposure. (**B**) Panel (1): ACh (a muscarinic receptor agonist) induced dilation coronary arterioles in sham-treated animals, but not in PM_{MTM}-exposed. Panel (2) Mesenteric arteriolar dilation was significantly inhibited following PM_{MTM} instillation compared with sham-treated animals. $^{*}p < 0.05$ vs. sham.

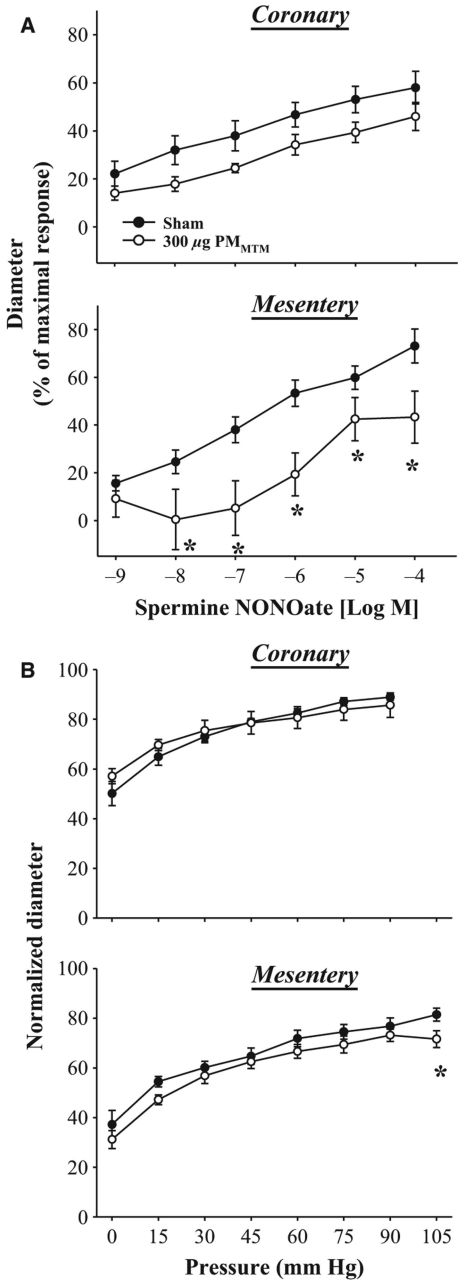

Figure 5.

Isolated arteriolar responsiveness to NO and transmural pressure. (**A**) Panel (1): PM_{MTM} treatment did not alter individual concentration points for Spermine NONOate; however, the overall response curves were different sham and PM_{MTM} IT groups. Panel (2): Mesenteric arteriolar dilation to Spermine NONOate was significantly inhibited following PM_{MTM}-treated compared with sham particle-treated. (**B**) Panel (1): Coronary arteriolar myogenic response was not altered following PM_{MTM} exposure. Panel (2): PM_{MTM} IT significantly enhanced arteriolar responsiveness to transmural pressure at 105 mmHg in mesenteric arterioles. *$p < 0.05$ vs. sham.

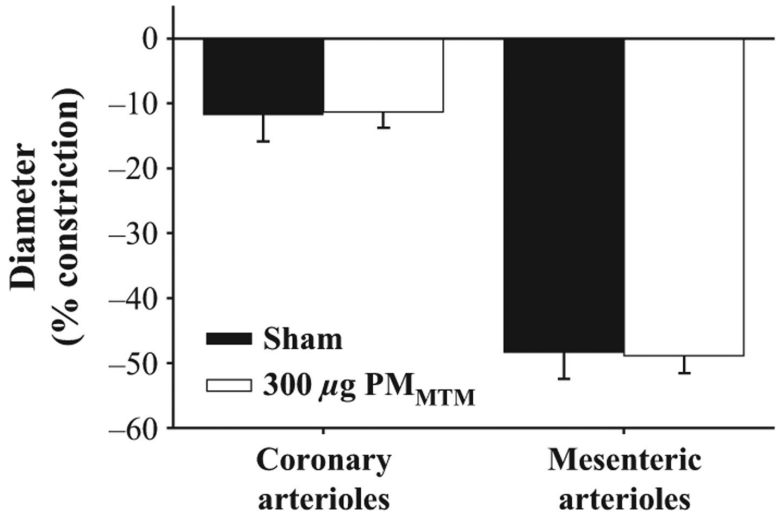

Figure 6.

Arteriolar constriction to PE (0.1 mM) was not significantly different between sham and MTM particle-treated groups in either microvascular bed.

Table 1

Animal characteristics

Experimental group	Animal number	Age (days)	Weight (g)	HR (bpm)	MAP (mmHg)
Intravital microscopy					
Sham	17	50 ± 1	270 ± 7	350 ± 7	92 ± 3
MTM	13	53 ± 2	266 ± 7	347 ± 10	92 ± 3
Isolated arterioles					
Sham	11	70 ± 2	386 ± 15	–	–
MTM	8	68 ± 3	345 ± 27	–	–

Table 2

ICP-AES, IC, OC/EC analysis

Element	*μ*g/mg Sample
Aluminum	1.29
Calcium	5.98
Iron	0.90
Potassium	1.58
Magnesium	0.69
Sodium	2.68
Titanium	0.18
Zinc	0.38
Sulfate	92.10
Organic carbon	274.60

Table 3

Vessel characteristics

	Sham			MTM		
	n	**Diameter (μm)**	**Tone (%)**	***n***	**Diameter**	**Tone**
Intravital microscopy						
Normal	44	36 ± 1	64 ± 1	29	38 ± 2	63 ± 2
L-NMMA	13	39 ± 2	61 ± 3	10	36 ± 2	69 ± 2 *
Phentolamine	9	35 ± 3	66 ± 3	8	37 ± 6	65 ± 6
ADO	45	103 ± 3	0	32	106 ± 3	0
Isolated arterioles						
Mesenteric	16	70 ± 4	30 ± 2	10	78 ± 3	25 ± 2
Ca^{++} free		99 ± 3	0		104 ± 2	0
Coronary	18	88 ± 4	24 ± 8	16	95 ± 8	30 ± 3
Ca^{++} free		116 ± 20	0		135 ± 10	0

* $p < 0.05$ vs. sham.